Inorg. Chem. **2004**, *43*, 6168–6176

Mono- and Dinuclear Complexes of Chiral Tri- and Tetradentate Schiff-Base Ligands Derived from 1,1′-Binaphthyl-2,2′-diamine

Shane G. Telfer,*,† Tomohiro Sato,† Takunori Harada,† Reiko Kuroda,*,†,‡ Julie Lefebvre,§ and Daniel B. Leznoff§

JST ERATO Kuroda Chiromorphology Project, Park Building, 4-7-6 Komaba, Meguro-ku, Tokyo, 153-0041 Japan, Graduate School of Arts and Sciences, University of Tokyo, Komaba, Meguro-ku, Tokyo, 153-8902 Japan, and Department of Chemistry, Simon Fraser University, 8888 University Drive, Burnaby, British Columbia, Canada V5A 1S6

Received January 22, 2004

The synthesis and characterization of the bis(bidentate) Schiff-base ligand [(*R*)-**2**] formed by the condensation reaction of (*R*)-1,1′-binaphthyl-2,2′-diamine [(*R*)-BINAM] with pyridine-2-carboxaldehyde is presented. The coordination chemistry of (*R*)-**2** with $Ni(ClO_4)_2 \cdot 6H_2O$, $Co(ClO_4)_2 \cdot 6H_2O$, $CuCl_2$, and $CuSO_4$ has been investigated. Reaction of (*R*)-**2** with the first two metal salts leads to complexes of the type $[M((R)\text{-}\mathbf{4})_2](ClO_4)_2$ ($M = Ni^{II}$, Co^{II}), where (*R*)-**4** is a tridentate ligand resulting from the hydrolytic cleavage of one of the pyridyl groups from (*R*)-**2**. Both complexes were characterized by X-ray crystallography, which showed that the Λ absolute configuration of the metal center is favored in both cases. ^{1}H NMR spectroscopy suggests that the high diastereoselectivity of Λ-$[Co((R)\text{-}\mathbf{4})_2](ClO_4)_2$ is maintained in solution. The reaction of (*R*)-**2** with $CuCl_2$ leads to the dinuclear complex $[Cu_2((R)\text{-}\mathbf{2})Cl_4]$, which has a $[Cu_2(\mu^2\text{-}Cl_2)]$ core. The reaction of $CuSO_4$ with (*R*)-**2** gives a dimeric complex, $\{Cu((R)\text{-}\mathbf{4})SO_4\}_2$, which features a $[Cu_2(\mu^2\text{-}(SO_4)_2)]$ core. This complex can be prepared directly by the reaction of (*R*)-BINAM with pyridine-2-carboxaldehyde and $CuSO_4$. The use of *rac*-BINAM in this synthetic procedure leads to the *heterochiral* dimer $[Cu_2((R)\text{-}\mathbf{4})((S)\text{-}\mathbf{4})(SO_4)_2]$; that is, the ligands undergo a self-sorting (self/nonself discrimination) process based on chirality. The reaction of *rac*-BINAM, pyridine-2-carboxaldehyde, and $Co(ClO_4)_2 \cdot 6H_2O$ proceeds via a *homochiral* self-sorting pathway to produce a racemic mixture of $[Co((R)\text{-}\mathbf{4})_2]^{2+}$ and $[Co((S)\text{-}\mathbf{4})_2]^{2+}$. The variable-temperature magnetic susceptibilities of the bimetallic complexes $[Cu_2((R)\text{-}\mathbf{2})Cl_4]$, $[Cu((R)\text{-}\mathbf{4})(\mu^2\text{-}SO_4)]_2$, and $[Cu_2((R)\text{-}\mathbf{4})((S)\text{-}\mathbf{4})(\mu^2\text{-}SO_4)_2]$ all show weak antiferromagnetic coupling with $J = -1.0$, -0.40, and -0.67 cm^{-1}, respectively.

Introduction

Chirality is central to coordination chemistry, and unites fields as diverse as asymmetric catalysis, bioinorganic chemistry, and supramolecular chemistry. The stereoselective synthesis of transition metal complexes represents a significant challenge to coordination chemists,[1] and one successful approach has been to use chiral ligands derived from building blocks such as amino acids,[2] amino alcohols,[3] and terpenes.[4] Where the metal center is stereogenic, the coordination of a chiral ligand will give rise to diastereoisomers. In general, the kinetic lability of the metal center ensures that these diastereoisomers are in rapid thermal equilibration, and often the energy difference between them is sufficient for one diastereomer to be formed exclusively.[1]

1,1′-Binaphthyl units that are functionalized at the 2- and 2′-positions are often chiral due to restricted rotation about the transannular bond. Though their importance in asymmetric synthesis cannot be overstated, chiral ligands based on binaphthyl frameworks have also found wide application in coordination and metallo-supramolecular chemistry.[5] A diverse range of binaphthyl starting materials are commercially available (or can be synthesized) in an enantiopure

* Author to whom correspondence should be addressed. E-mail: shane.telfer@chiromor2.erato.rcast.u-tokyo.ac.jp. Fax/Tel: +81 3 5465 0104.

† JST ERATO Kuroda Chiromorphology Project.

‡ University of Tokyo.

§ Simon Fraser University.

(1) Knof, U.; von Zelewsky, A. *Angew. Chem., Int. Ed.* **1999**, *38*, 303−322.

(2) Telfer, S. G.; Bernardinelli, G.; Williams, A. F. *Chem. Commun.* **2001**, 1498−1499.

(3) Telfer, S. G.; Kuroda, R.; Sato, T. *Chem. Commun.* **2003**, 1064−1065.

(4) von Zelewsky, A.; Mamula, O. *J. Chem. Soc., Dalton Trans.* **2000**, 219−231.

(5) Telfer, S. G.; Kuroda, R. *Coord. Chem. Rev.* **2003**, *242*, 33−46.

10.1021/ic049910y CCC: $27.50
Published on Web 08/18/2004

Scheme 1. Synthetic Route to Ligands **1** and **2** and the Structures of Ligands **3** and **4**

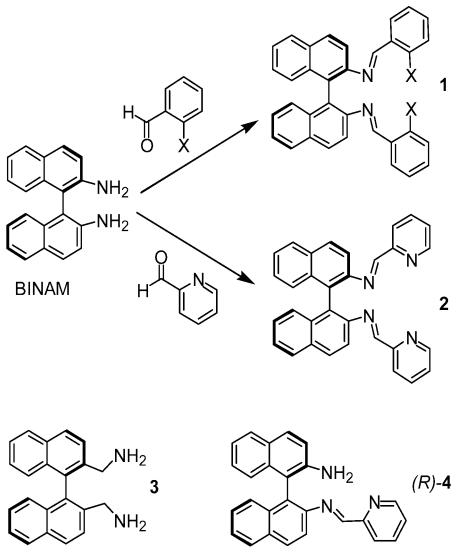

form, and these can be readily functionalized with a variety of donor groups. One example of a highly versatile starting material is 1,1′-binaphthyl-2,2′-diamine (BINAM). A large number of Schiff-base ligands (**1**) can be prepared by simply capping the free amino groups with suitable aldehydes (Scheme 1). Salicaldimine derivatives have been particularly well-studied (**1**, X = OH) and have found applications in asymmetric catalysis[6] and biomimetic chemistry.[7] In contrast, pyridylimine derivatives such as **2** have received scant attention. Hannon's group have shown that ligand **2** reacts with Cu(I) and Ag(I) to give $[M_2(\mathbf{2})_2]^{2+}$ helicates.[8] These helicates were formed with very high diastereoselectivity; that is, the chirality of the ligand controls the handedness of the helicate. In the only other literature report featuring ligand **2**, it has been shown that its Ir(I), Rh(I), and Ti(IV) complexes are useful catalysts for a range of asymmetric transformations, though these complexes were not well characterized.[9]

We have recently launched a research program focusing on ligands derived from BINAM and the related amine **3**. One of our initial aims has been to further explore the coordination chemistry of ligand **2**. In particular, we wanted to investigate its reactions with metal ions that prefer nontetrahedral coordination geometries. In this report, we present some observations concerning the chemistry of ligand **2** with a variety of Co(II), Ni(II), and Cu(II) salts. We have found ligand **2** to be very sensitive to hydrolysis, and as a result, the majority of complexes that we were able to isolate actually contained the tridentate ligand **4**.

Results and Discussion

Synthesis and Characterization of Ligand 2. Previous work concerning the coordination chemistry ligand **2** relied on its in situ formation in the presence of the coordinating metal ions. We were, however, able to prepare ligand **2** directly by mixing BINAM and pyridine-2-carboxaldehyde in dry CH_2Cl_2 in the presence of molecular sieves. The reaction appears to be essentially quantitative; therefore, if the reagents are combined with an exact 1:2 stoichiometry, the product can be isolated in high yield simply by removing the molecular sieves and the solvent. The resulting yellow solid was characterized by ^{1}H NMR, ^{13}C NMR, electrospray mass spectrometry (ES-MS), UV−visible spectroscopy, circular dichroism (CD) spectroscopy, and elemental analysis.

Reaction of 2 with $Co(ClO_4)_2\cdot 6H_2O$ and $Ni(ClO_4)_2\cdot 6H_2O$. As outlined above, ligand **2** reacts with Cu(I) and Ag(I) salts to form dinuclear double-stranded helicates $[M_2L_2]^{2+}$.[8] In these complexes the ligand coordinates in a bridging bis(bidentate) fashion. We were interested to see whether this coordination mode would also be operative when ligand **2** binds to a metal center that has a preference for an octahedral coordination geometry. If this coordination mode was maintained, we may expect that a dinuclear triple-stranded helicate $[M_2L_3]^{2+}$ will form.

A solution of $Ni(ClO_4)_2\cdot 6H_2O$ was titrated into a solution of (*R*)-**2** in CH_3OH, and the changes in the composition of the solution were monitored by ES-MS. Initially, the spectrum showed peaks at m/z = 463.2 and 491.2, which can be assigned to $[\mathbf{2}H]^+$ and $[Ni(\mathbf{2})_2]^{2+}$, respectively. From a Ni/**2** ratio of around 2/5 onward, two other peaks gradually grew into the spectrum at m/z = 260.1 and 619.1. These peaks can be attributed to $[Ni(\mathbf{2})]^{2+}$ and $[Ni(\mathbf{2})(ClO_4)]^+$, respectively. These were the only peaks visible when the Ni/**2** ratio reached 1/1. No peaks due to any polynuclear species such as $[Ni_2(\mathbf{2})_3]^{2+}$ were visible at any point throughout the titration.

Similar results were observed when $Co(ClO_4)_2\cdot 6H_2O$ was used in place of $Ni(ClO_4)_2\cdot 6H_2O$, with a peak due to $[Co(\mathbf{2})_2]^{2+}$ appearing at low Co/**2** ratios and peaks corresponding to $[Co(\mathbf{2})]^{2+}$ and $[Co(\mathbf{2})(ClO)_4]^+$ dominating the ES-MS spectrum at higher Co/**2** ratios. A ^{1}H NMR titration was also performed with CD_3CN as the solvent. The diamagnetic peaks due to the free ligand gradually disappeared as $Co(ClO_4)_2\cdot 6H_2O$ was titrated into the solution and were replaced by a large number of peaks, paramagnetically shifted over a range of 150 ppm. The change in the relative intensities of these paramagnetic peaks as the titration progressed showed that at least two distinct complexes were formed. We tentatively assign these sets of peaks to the complexes $[Co(\mathbf{2})_2]^{2+}$ and $[Co(\mathbf{2})]^{2+}$; however, the spectra were too complex to allow a more certain characterization.

The complexity of the ^{1}H NMR spectrum at a Co/**2** ratio of 1/1 may arise from the presence of multiple isomers of $[Co((R)\text{-}\mathbf{2})]^{2+}$. To cast some light on this situation, we attempted to grow crystals of both this complex and its nickel(II) analogue for analysis by X-ray crystallography. An orange-red solution of $Ni(ClO_4)_2\cdot 6H_2O$ and (*R*)-**2** (1/1 ratio) was prepared in CH_3NO_2, and diethyl ether was slowly diffused into this solution. Red block-shaped crystals formed

(6) Che, C.-M.; Huang, J.-S. *Coord. Chem. Rev.* **2003**, *242*, 97−113.
(7) Wang, Y.; DuBois, J. L.; Hedman, B.; Hodgson, K. O.; Stack, T. D. P. *Science* **1998**, *279*, 537.
(8) Hamblin, J.; Childs, L. J.; Alcock, N. W.; Hannon, M. J. *J. Chem. Soc., Dalton Trans.* **2002**, 164−169.
(9) Guo-Fu, Z.; Cheng-Lie, Y. *J. Mol. Catal. A* **1998**, *132*, L1-L4.

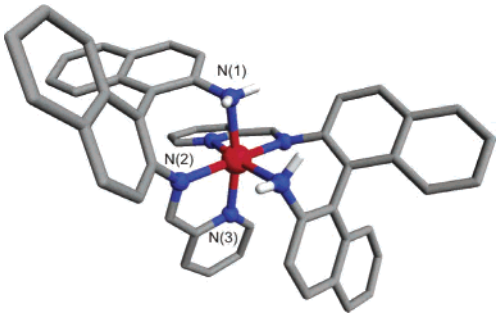

Figure 1. X-ray crystal structure of the $[Ni((R)\text{-}\mathbf{4}_2)]^{2+}$ cation. Red = Ni; blue = N; gray = C; white = H. Hydrogen atoms, except those of the amine nitrogens, have been omitted for clarity. A crystallographic C_2 axis relates the two halves of the cation. Selected distances (in angstroms): N(1)−Ni, 2.162(4); N(2)−Ni, 2.079(4); N(3)−Ni, 2.106(4). Selected angles (in degrees): N(1)−Ni−N(2), 90.1(1); N(2)−Ni−N(3), 79.1(1).

after several days, and analysis of these crystals by X-ray crystallography revealed the structure shown in Figure 1. It can be seen that ligand (*R*)-**2** has lost one of its pyridyl groups due to hydrolysis of one of its azomethine bonds. Two molecules of the resulting tridentate ligand (*R*)-**4** coordinate to the nickel(II) center to give a complex $[Ni((R)\text{-}\mathbf{4}_2](ClO_4)_2{\cdot}CH_3NO_2$.

The nickel(II) center of the $[Ni((R)\text{-}\mathbf{4}_2]^{2+}$ cation adopts a distorted octahedral geometry, with Ni−N bond lengths in the range 2.08−2.16 Å. These bonds are of similar length to those observed in other nickel(II) complexes with N-donor ligands such as $[Ni(bipy)_3]^{2+}$ (2.08−2.10 Å)[10] and $[Ni(en)_3]^{2+}$ (2.13−2.14 Å),[11] though slightly longer than those in a related Ni(II)−pyridylimine complex.[12] The torsion angle between the two naphthyl planes of the ligand is 112.5°. One of the perchlorate counterions is disordered over two symmetry-related sites. Close contacts between its oxygen atoms and N(1) of the complex (N···O = 2.10 and 2.47 Å) are indicative of hydrogen-bonding interactions.

$[Ni((R)\text{-}\mathbf{4}_2](ClO_4)_2$ could also be synthesized in good yield by combining (*R*)-BINAM, pyridine-2-carboxaldehyde, and $Ni(ClO_4)_2{\cdot}6H_2O$ directly in CH_3OH. This enabled characterization of the complex by microanalysis and IR, UV−vis, and ES-MS spectroscopy.

The corresponding cobalt(II) complex could be prepared in a similar fashion by use of $Co(ClO_4)_2{\cdot}6H_2O$ as a starting material. Large red crystals formed in the reaction mixture, and X-ray crystallography showed that the $[Co((R)\text{-}\mathbf{4}_2](ClO_4)_2$ complex had indeed formed. In this case, free BINAM was found to have cocrystallized with the complex (Figure 2). The structure of the $[Co((R)\text{-}\mathbf{4}_2]^{2+}$ cation is broadly similar to its nickel(II) analogue, though the former complex lacks a crystallographic C_2 axis and the geometries of its two ligands are somewhat different. Four of the Co−N bond lengths fall in the range 2.14−2.19 Å, which is comparable to the bond lengths in $[Co(bipy)_3]^{2+}$ (2.09−2.15 Å)[13] and $[Co(en)_3]^{2+}$ (2.10−2.17 Å).[14] The remaining Co−NH_2 bond is relatively long (2.238 Å) and can be ascribed

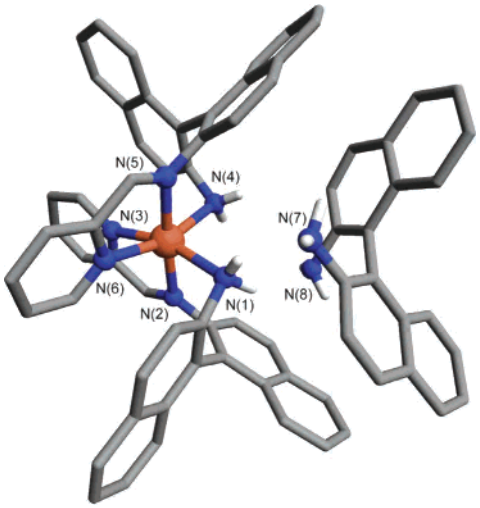

Figure 2. $[Co((R)\text{-}\mathbf{4}_2)]^{2+}$ cation and free BINAM of the X-ray crystal structure of $[Co((R)\text{-}\mathbf{4}_2](ClO_4)_2{\cdot}BINAM{\cdot}(CH_3OH)_2$. Orange = Co; blue = N; gray = C; white = H. Hydrogen atoms, except those of the amine nitrogens, have been omitted for clarity. Selected distances (in angstroms): N(1)−Co, 2.238(3); N(2)−Co, 2.167(2); N(3)−Co, 2.139(3); N(4)−Co, 2.192(3); N(5)−Co, 2.168(3); N(6)−Co, 2.136(2); N(1)−N(7), 3.493; N(4)−N(7), 3.143; N(4)−N(8), 3.024. Selected angles (in degrees): N(1)−Co−N(2), 90.7(1); N(1)−Co−N(4), 97.1(1); N(2)−Co−N(3), 76.3(1).

to hydrogen bonding to the free BINAM molecule. These hydrogen bonds are indicated by the close contact of N(4) with both N(7) and N(8) (N···N = 3.143 and 3.042 Å, respectively), and of N(1) with N(7) (N···N = 3.493 Å).

The ^1H NMR spectrum of $[Co((R)\text{-}\mathbf{4}_2](ClO_4)_2$ was recorded in CD_3NO_2. A total of 13 peaks, paramagnetically shifted over a range of 100 ppm, appeared in the spectrum. A total of 19 magnetically distinct protons are expected if the C_2 symmetry of the $[Co((R)\text{-}\mathbf{4}_2]^{2+}$ is retained in solution. Integration of the spectrum showed that the observed peaks account for 15 of these protons, and we suspect that the signals of the remaining protons are rendered invisible by extreme paramagnetic line broadening (in particular the two amine protons). The ES-MS spectrum of $[Co((R)\text{-}\mathbf{4}_2](ClO_4)_2$ dissolved in CH_3OH is also consistent with the retention of the solid-state structure in solution, showing peaks assignable to $[Co((R)\text{-}\mathbf{4}_2]^{2+}$ (*m*/*z* 402.5) and $[Co((R)\text{-}\mathbf{4}_2(ClO_4)]^+$ (*m*/*z* 904).

Ligand **4** is tridentate and therefore, in theory, can bind in either facial or meridional mode. Molecular models indicate, however, that the facial binding mode would be highly disfavored due steric constraints imposed by the binaphthyl unit. Indeed, the meridional binding mode is observed in the X-ray crystal structures of $[Co((R)\text{-}\mathbf{4}_2](ClO_4)_2$ and $Ni((R)\text{-}\mathbf{4}_2](ClO_4)_2$.

When tridentate ligands that possess a C_2 symmetry axis (e.g., terpyridine) coordinate to an octahedral metal center to give an $[M(ABA)_2]$ complex (ABA = C_2-symmetric tridentate ligand), no new elements of symmetry are formed. On the other hand, when ligands that lack a C_2 symmetry axis (ABC) coordinate to an octahedral metal center to give a $[M(ABC)_2]$ complex, the metal center becomes stereogenic.

(10) Wada, A.; Sakabe, N.; Tanaka, J. *Acta Crystallogr. B* **1976**, *32*, 1121.
(11) Chestnut, D. J.; Haushalter, R. C.; Zubieta, J. *Inorg. Chim. Acta* **1999**, *292*, 41.
(12) Tuna, F.; Clarkson, G.; Alcock, N. W.; Hannon, M. J. *Dalton Trans.* **2003**, 2149−2155.
(13) Szalda, D. J.; Creutz, C.; Mahajan, D.; Sutin, N. *Inorg. Chem.* **1983**, *22*, 2372−2379.
(14) Stephan, H.-O.; Kanatzdis, M. G. *J. Am. Chem. Soc.* **1996**, *118*, 12226.

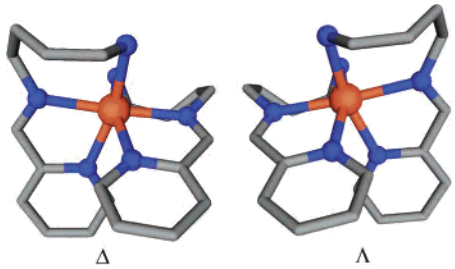

Figure 3. Two enantiomers of a *mer*-[M(ABC)$_2$] complex, with the core of the [Co((*R*)-**4**)$_2$]$^{2+}$ complex as an example.

This kind of chirality has parallels in tetrahedral complexes of the type [M(AB)$_2$] and in certain organic spiro compounds.[15] The two enantiomers of a [M(ABC)$_2$] complex are shown schematically in Figure 3 with the core of the [Co((*R*)-**4**)$_2$]$^{2+}$ complex as an example. These enantiomers may be assigned either Δ- or Λ- stereochemical descriptors according to the oriented line reference system.[16] From the X-ray crystal structures of [Co((*R*)-**4**)$_2$](ClO$_4$)$_2$ and Ni((*R*)-**4**)$_2$](ClO$_4$)$_2$, it can be seen that both complexes adopt the Λ configuration. Thus, the axial chirality of the ligand efficiently predetermines the stereochemistry of the metal centers in the solid state. As outlined above, ^{1}H NMR spectroscopy indicates that this diastereoselectivity is maintained in solution.

Reaction of 2 with CuCl$_2$. The addition of a solution of (*R*)-**2** in dry CH$_2$Cl$_2$ to a solution of CuCl$_2$ in dry CH$_3$OH led to the precipitation of a yellow-brown solid. Dark brown crystals could be obtained by the slow diffusion of ^{t}BuOMe into a solution of the complex in CH$_2$Cl$_2$/CH$_3$OH, and X-ray crystallography revealed the complex [Cu$_2$((*R*)-**2**)Cl$_4$] (Figure 4). In this structure, the ligand cradles a planar, rhomboidal [Cu$_2$(μ^2-Cl$_2$)] unit. A nonbridging chloro ligand completes the coordination sphere of each copper center. The overall structure has a pseudo-C_2 axis running perpendicular to the [Cu$_2$Cl$_2$] plane. To accommodate the [Cu$_2$Cl$_2$] unit, the binaphthyl framework adopts an open structure (naphthyl−naphthyl torsion angle = 78.5°), and the pyridyl−imine chelates are rotated out of the naphthyl planes (pyridyl−imine−naphthyl torsion angle = 60.1°). This unit is asymmetric with one short basal Cu−Cl bond (average 2.259 Å) and one long apical Cu−Cl bond (average 2.605 Å). The Cu···Cu separation is 3.495 Å. The geometry of the copper(II) centers is intermediate between square pyramidal and trigonal bypyramidal. This is more precisely described by Reedijk's τ factor, which averages 0.36 (τ = 0 for exact square pyramidal and τ = 1 for exact trigonal bypyramidal).[17]

Complexes that feature a [Cu$_2$(μ-Cl)$_2$] moeity have been reported frequently in the literature, the Cambridge Crystallographic Database containing 478 examples.[18] More than half of these can be grouped togther with [Cu$_2$((*R*)-**2**)Cl$_4$] in a class of [Cl(L)Cu(μ^2-Cl)$_2$Cu(L)Cl] complexes in which a

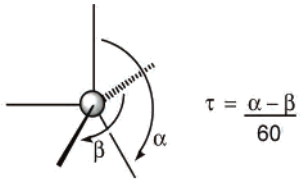

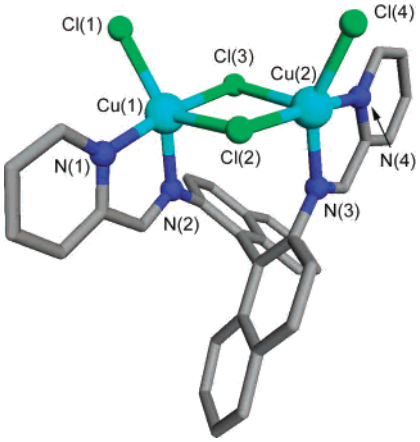

Figure 4. X-ray crystal structure of [Cu$_2$((*R*)-**2**)Cl$_4$]. Selected distances (in angstroms): Cu(1)−Cl(1), 2.225(1); Cu(1)−Cl(2), 2.606(1); Cu(1)−Cl(3), 2.266(1); Cu(1)−N(1), 2.005(4); Cu(1)−N(2), 2.053(4); Cu(2)−Cl(1), 2.254(1); Cu(2)−Cl(2), 2.605(1); Cu(2)−Cl(3), 2.26(1); Cu(2)−N(3), 2.070(4); Cu(2)−N(4), 2.009(4); Cu(1)···Cu(2), 3.495. Bond angles (in degrees): Cl(2)−Cu(1)−Cl(3), 87.95(4); Cl(2)−Cu(2)−Cl(3), 88.22(4); Cu(1)−Cl(2)−Cu(2), 91.69(4); Cu(1)−Cl(3)−Cu(2), 91.43(4).

nonbridging chloro ligand is also found in the coordination sphere of each metal center. (In a large proportion of the remaining structures, the [Cu$_2$(μ^2-Cl)$_2$] unit is found as part of the [Cu$_2$Cl$_6$]$^{2-}$ anion.) A close examination of this group of [Cl(L)Cu(μ^2-Cl)$_2$Cu(L)Cl] complexes reveals that the syn orientation of the nonbridging chloro ligands, as seen in [Cu$_2$((*R*)-**2**)Cl$_4$], is quite rare. It appears that only three other complexes with this structural motif have been crystallographically characterized.[19] Typically, these nonbridging chloro ligands are arranged in an anti fashion or are coplanar with the [Cu$_2$(μ-Cl)$_2$] unit.

Reaction of 2 with CuSO$_4$. Ligand (*R*)-**2** was combined with 1 equiv of anhydrous CuSO$_4$ in dry MeOH and the reaction mixture was warmed to 50 °C in a closed vial for several days. Large brown crystals formed, and X-ray crystallographic analysis revealed the structure shown in Figure 5. This complex is a copper(II) dimer, {Cu((*R*)-**4**)(μ^2-SO$_4$)}$_2$, which contains ligand (*R*)-**4**. Presumably ligand (*R*)-**2** was hydrolyzed to give (*R*)-**4** by atmospheric H$_2$O that permeated the vial.

The {Cu((*R*)-**4**)(μ^2-SO$_4$)}$_2$ dimer has crystallographically imposed C_2 symmetry that relates the two monomeric halves of the complex. The core of this complex comprises a [Cu$_2$(μ^2-SO$_4$)$_2$] unit, which has Cu−O bond distances of 1.970 and 2.178 Å, and a Cu···Cu separation of 4.759 Å. (*R*)-**4**

(15) Eliel, E. L.; Wilen, S. H.; Mander, L. N. *Stereochemistry of Organic Compounds*; Wiley: New York, 1994.
(16) von Zelewsky, A. *Stereochemistry of Coordination Compounds*; Wiley: Chichester, U.K., 1996.
(17) Addison, A. W.; Rao, T. N.; Reedijk, J.; Rijn, J. V.; Verschoor, G. C. *J. Chem. Soc., Dalton Trans.* **1984**, 1349.
(18) CSD Version 5.24 (November 2002).
(19) (a) Mandel, S. K.; Thompson, L. K.; Newlands, M. J.; Yee, F. L.; Lepage, Y.; Charland, J.-P.; Gabe, E. J. *Inorg. Chim. Acta* **1986**, *122*, 199. (b) Chen, L.; Thompson, L. K.; Bridson, J. N. *Inorg. Chem.* **1993**, *32*, 2938.

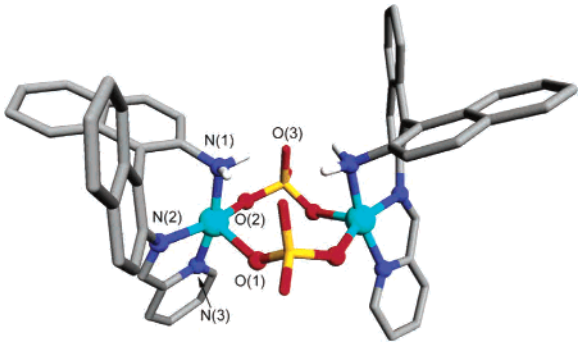

Figure 5. X-ray crystal structure of {Cu((*R*)-**4**)(μ^2-SO_4)}$_2$. All hydrogen atoms, except those of the amine nitrogens, have been omitted for clarity. The Cu centers are shown as blue-green spheres. Distances (in angstroms): Cu−O(1), 2.178(2); Cu−O(2), 1.970(2); Cu−N(1), 2.000(2); Cu−N(2), 2.056(2); Cu−N(3), 2.005(3); N(1)−O(3), 2.790; Cu···Cu, 4.759; S···S, 4.449. Bond angles (in degrees): O(1)−Cu−O(2), 105.87(8); N(1)−Cu−N(3), 166.9(1); N(2)−Cu−O(1), 91.93(9); N(2)−Cu−O(2), 160.75(9).

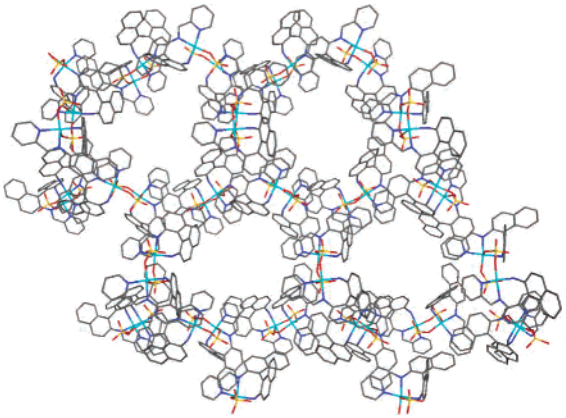

Figure 6. Packing diagram showing the large channels in the crystal structure of the {Cu((*R*)-**4**)(μ^2-SO_4)}$_2$ dimer (viewed down the crystallographic *c* axis). The colors of the atoms correspond to those in Figure 5.

acts as a tridentate ligand, coordinating to each copper center in a meridional fashion. The geometry of the five coordinate copper centers is slightly distorted from square pyramidal (τ value = 0.102). The N(1), N(2), N(3), and O(2) atoms define the basal plane (RMS deviation = 0.0464 Å), and the O(1) center represents the apex of the pyramid. The copper center lies 0.264 Å out of the basal plane toward the apical oxygen atom. The μ^2-SO_4^{2-} ligands can be described as bridging in a basal−apical fashion; that is, one oxygen atom occupies a basal site of one copper center with another oxygen occupying the apical site of the second copper center. Short internuclear contacts between the amine nitrogen atoms and the noncoordinating sulfate oxygen atoms (2.786 and 2.793 Å) are indicative of hydrogen-bonding interactions and are discussed further below.

A view of the packing diagram of {Cu((*R*)-**4**)(μ^2-SO_4)}$_2$ down the crystallographic *c* axis is presented in Figure 6. This reveals remarkably large pores in the crystal with diameters of around 12 Å. The channels are lined by binaphthyl and pyridyl residues and appear to be filled with solvent (CH_3OH) molecules. The presence of these pores accounts for the rapid loss of crystallinity upon the removal of these crystals from solution. Another notable feature of the extended structure of this complex is the existence of intermolecular face-to-face $\pi-\pi$ interactions between both

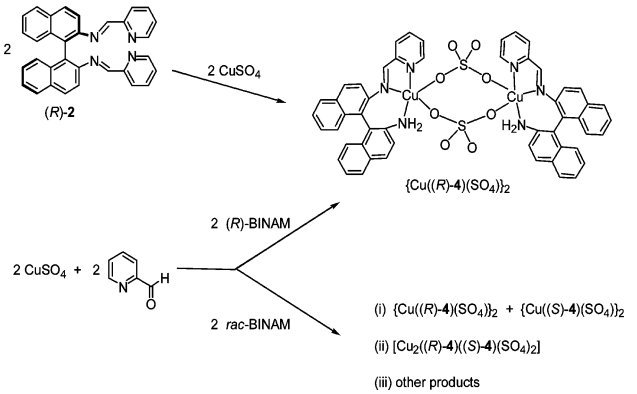

Figure 7. Two synthetic pathways to the formation of the {Cu(**4**)(μ-SO_4}$_2$ dimer and a summary of the various possible stereochemical outcomes of the reaction if *rac*-BINAM is used as a starting material.

pyridyl groups of each complex with binaphthyl rings of two different neighboring complexes. There is near-total overlap of the two rings, and the C···C distances are in the range 3.45−3.74 Å.

Ligand Self-Sorting Based on Chirality. The {Cu((*R*)-**4**)(μ^2-SO_4)}$_2$ dimer can be prepared directly in good yield by combining (*R*)-BINAM, pyridine-2-carboxaldehyde, and $CuSO_4$·$5H_2O$ in MeOH (Figure 7). In this case, a homochiral dimer (i.e., one in which the two ligands have the same chirality) must form because enantiopure BINAM was used as a starting material. What happens if racemic BINAM is used in place of enantiopure BINAM?

We may envisage three possible outcomes to this reaction, as depicted in Figure 7: (i) A racemic mixture of the homochiral dimers {Cu((*R*)-**4**)(μ^2-SO_4)}$_2$ and {Cu((*S*)-**4**)(μ^2-SO_4)}$_2$ may form; (ii) the heterochiral dimer [Cu_2((*R*)-**4**)-((*S*)-**4**)(μ^2-SO_4)$_2$] may form; or (iii) an entirely different product may form. There are a number of reports in the literature concerning similar systems, and all three reaction pathways noted above have been observed.[2,20]

If the first reaction pathway is followed to give the homochiral complex, the ligands must be capable of a highly efficient self-recognition process. Alternatively, formation of a heterochiral complex implies that the ligands undergo a self/nonself discrimination process. These self-sorting phenomena, which are based solely on the chirality of the ligands, can be viewed in the broader context of general self-sorting phenomena.[21]

This experiment involving racemic BINAM was performed by combining 1 equiv each of *rac*-BINAM, pyridine-carboxaldehyde, and $CuSO_4$·$5H_2O$ in MeOH. A mass of small dark brown crystals gradually formed in high yield (90%) upon allowing the reaction mixture to sit in a closed vial at 50 °C. Crystals suitable for X-ray crystallography were grown by the slow diffusion of Et_2O into a solution of the crude product dissolved in MeOH. The X-ray crystal

(20) (a) Rowland, J. M.; Olmstead, M. M.; Mascharak, P. K. *Inorg. Chem.* **2002**, *41*, 1545−1549. (b) Provent, C.; Bernardinelli, G.; Williams, A. F.; Vulliermet, N. *Eur. J. Inorg. Chem.* **2001**, 1963−1967. (c) Kim, T. W.; Lah, M. S.; Hong, J.-I. *Chem. Commun.* **2001**, 743−744. (d) Masood, M. A.; Enemark, E. J.; Stack, T. D. P. *Angew. Chem., Int. Ed.* **1998**, *37*, 928−932. (e) Kondo, T.; Oyama, K.-i.; Yoshida, K. *Angew. Chem., Int. Ed.* **2001**, *40*, 894.
(21) Wu, A.; Isaacs, L. *J. Am. Chem. Soc.* **2003**, *125*, 4831−4835.

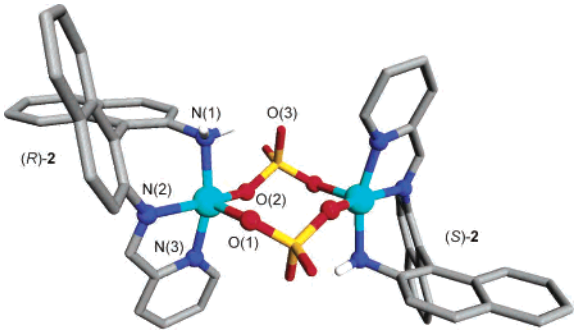

Figure 8. X-ray crystal structure of the heterochiral [Cu_2((*R*)-**4**)((*S*)-**4**)(μ^2-SO_4)$_2$] complex. All hydrogen atoms, except those of the amine nitrogens, have been omitted for clarity. The Cu centers are represented as blue-green spheres. Distances (in angstroms): Cu−O(1), 2.131(1); Cu−O(2), 1.965(1); Cu−N(1), 2.023(2); Cu−N(2), 2.046(2); Cu−N(3), 2.004(2); N(1)−O(3), 2.758; Cu···Cu, 4.801; S···S, 4.270. Bond angles (in degrees): O(1)−Cu−O(2), 107.04(6); N(1)−Cu−N(3), 161.59(7); N(2)−Cu−O(1), 93.33(6); N(2)−Cu−O(2), 158.74(6).

structure (Figure 8) shows that the *heterochiral* (or meso) dimer [Cu_2((*R*)-**4**)((*S*)-**4**)(μ^2-SO_4)$_2$], containing a crystallographic center of inversion, is formed. (The structure of this complex is discussed further below.) Microanalysis and magnetic measurements (vide infra) confirm that this crystal is representative of the bulk material and, importantly, confirm that this compound is distinct from its homochiral analogue. The insolubility of [Cu_2((*R*)-**4**)((*S*)-**4**)(μ^2-SO_4)$_2$ prevented its characterization in solution; therefore, we are unable to state with confidence whether it is thermodyamically favored over its homochiral counterpart *or* whether it is isolated from the reaction mixture because it is less soluble.

On the other hand, ^{1}H NMR spectroscopy clearly indicates that Λ-[Co((*R*)-**4**)$_2$]$^{2+}$ and Δ-[Co((*S*)-**4**)$_2$]$^{2+}$ are the thermodynamically favored products when *rac*-BINAM, pyridine-2-carboxaldehyde, and $Co(ClO_4)_2$ are combined, the ^{1}H NMR spectrum of the complexes isolated from this mixture being identical to that of Λ-[Co((*R*)-**4**)$_2$](ClO_4)$_2$. Thus, the ligands are capable of self-sorting, and the complexation reaction proceeds via the *homochiral* pathway (i).

Comparison of the Structures of the Homo- and Heterochiral Copper(II) Dimers. The structure of the heterochiral dimer, [Cu_2((*R*)-**4**)((*S*)-**4**)(μ^2-SO_4)$_2$], can be compared with that of the homochiral dimer, {Cu((*R*)-**4**)(μ^2-SO_4)}$_2$. A close-up view of the cores of the two complexes is presented in Figure 9.

It is noteworthy that the μ^2-SO_4^{2-} ligands in both complexes bridge in a basal−apical fashion. Also, the coordination spheres of the copper centers of the two complexes are nearly congruent. There is, however, a striking difference in the relative dispositions of the nitrogen ligands (**4**). For the heterochiral dimer, the amine groups of **4** adopt an anti arrangement; that is, they are on opposite sides of the [Cu−SO_4−Cu−SO_4] ring. On the other hand, a syn arrangement of the amine groups of **4** is observed for the homochiral dimer. In both complexes, it appears that hydrogen bonding between these amine groups and the sulfate oxygen centers is significant. The relative arrangement of the amine groups in {Cu((*R*)-**4**)(μ^2-SO_4)}$_2$ allows for the formation of four hydrogen bonds, while only two hydrogen bonds are able to form in [Cu_2((*R*)-**4**)((*S*)-**4**)(μ^2-SO_4)$_2$].

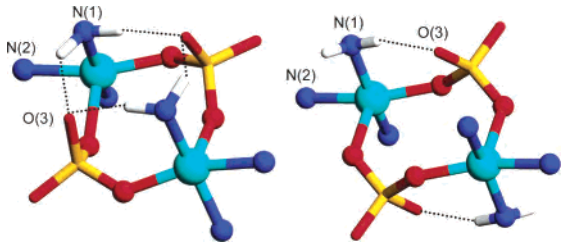

Figure 9. Close-up view of the cores of the {Cu((*R*)-4)(μ^2-SO_4)}$_2$ (left) and [Cu_2((*R*)-4)((*S*)-4)(μ^2-SO_4)$_2$] (right) dimers. The dotted lines indicate hydrogen bonds.

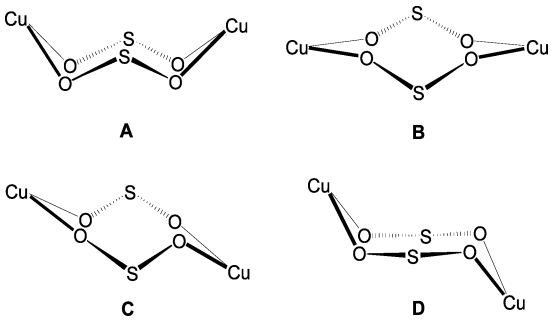

Figure 10. Schematic of the various conformations of the [Cu_2(μ^2-SO_4)$_2$] moiety that have been characterized by X-ray crystallography.

Consequently, the conformations of the [$Cu_2(SO_4)_2$] cores of the two complexes are rather different. These conformations are depicted schematically in Figure 10.

{Cu((*R*)-**4**)(μ^2-SO_4)}$_2$ adopts the butterfly or W-shaped conformation (labeled A) in which the ligating oxygen atoms describe a plane that lies below the plane described by the copper and sulfur atoms. On the other hand, [Cu_2((*R*)-**4**)((*S*)-**4**)(μ^2-SO_4)$_2$] is found in the boatlike conformation B, where the copper and oxygen atoms lie (nearly) in the same plane, with the sulfur centers located above and below this plane.

Four other complexes that feature a [Cu_2(μ^2-SO_4)$_2$] core have been reported in the literature. Of these complexes, one also adopts conformation B ({Cu(oaoH$_2$)(H_2O)SO_4}$_2$),[22] two adopt conformation C ([Cu(PAHOX)(SO_4)]$_2$·2H_2O and [Cu_4(pytp)$_2$(SO_4)$_2$(H_2O)$_{10}$](SO_4)$_2$·4H_2O),[23] and one adopts the chairlike conformation D ({Cu(mde)SO_4}$_2$).[24,25] It is noteworthy that intramolecular hydrogen bonding involving the sulfate groups is also present in the complex that was found in conformation B ({Cu(oaoH$_2$)(H_2O)SO_4}$_2$).[22] For all of the complexes that adopt conformations A−C, the μ^2-SO_4 ligands are all found to bridge the copper centers in a basal−apical fashion. On the other hand, for the complex which was found in arrangement D, {Cu(mde)SO_4}$_2$, both sulfate bridges link two *basal* sites of the copper centers.[24] The

(22) Endres, H.; Nothe, D.; Rossato, E.; Hatfield, W. E. *Inorg. Chem.* **1984**, *23*, 3467−3473.
(23) (a) Thompson, L. K.; Xu, Z.; Goeta, A. E.; Howard, J. A. K.; Clase, H. J.; Miller, D. O. *Inorg. Chem.* **1998**, *37*, 7. (b) Zou, X.-H.; Cai, J.-W.; Feng, X.-L.; Hu, X.-P.; Yang, G.; Zhang, H.; Ji, L.-N. *Trans. Met. Chem.* **2001**, *26*, 704−708.
(24) Arnold, P. J.; Davies, S. C.; Dilworth, J. R.; Durrant, M. C.; Griffiths, D. V.; Hughes, D. L.; Richards, R. L.; Sharpe, P. C. *J. Chem. Soc., Dalton Trans.* **2001**, 736−746.
(25) oaoH2 = oxamide oxime; PAHOX = a polydentate diazine ligand; pytp = [3-(2-pyridyl)-triazino[5,6-*f*]1,10-phenanthroline; mde = 2-(methylsulfanyl)-1,1-di(2-pyridyl)ethylamine.

Cu−O bonds in this complex are therefore both relatively short (average 1.949 Å). This in turn leads to a Cu···Cu distance (4.122 Å) that is significantly shorter than in the other complexes (4.76−5.09 Å).

Magnetic Properties. The temperature (T) dependence of the molar magnetic susceptibility (χ_M) of polycrystalline samples of $[Cu_2((R)\text{-}\mathbf{2})Cl_4]$, $[Cu((R)\text{-}\mathbf{4})(\mu^2\text{-}SO_4)]_2$, and $[Cu_2((R)\text{-}\mathbf{4})((S)\text{-}\mathbf{4})(\mu^2\text{-}SO_4)_2]$ were measured in the temperature range 1.8−300 K. All three samples show Curie law behavior (temperature-independent μ_{eff}) for the majority of the temperature range. For example, for the copper chloride-bridged dimer $[Cu_2((R)\text{-}\mathbf{2})Cl_4]$, $\mu_{eff} = 1.8\mu_B$ (per copper center) at 300 K, consistent with isolated $S = {}^1/_2$ copper(II) centers. The μ_{eff} value remains constant until 35 K, at which point it begins to decrease, reaching a value of $\mu_{eff} = 1.28\mu_B$ at 1.8 K. There is no maximum in the χ_M vs T plot. This behavior is consistent with the presence of weak antiferromagnetic interactions. By use of the Bleaney−Bowers[26] dimer model (with $H = -2JS_1 \cdot S_2$) to fit these weak intradimer interactions, the best-fit values of $J = -1.04 \pm 0.02$ cm^{-1} and $g = 2.000 \pm 0.006$ are obtained. This weak coupling between the two copper(II) centers in $[Cu_2((R)\text{-}\mathbf{2})Cl_4]$ can be attributed to the basal/apical geometry of the chloro bridges; such an arrangement has been shown both experimentally[27] and theoretically[28] to lead to minimal orbital overlap and consequently weak coupling. A study of a series of compounds with axial−equatorial $\{Cu(\mu\text{-}Cl)_2Cu\}$ cores yielded a magnetostructural correlation based on the Cu−Cl−Cu angle,[27] which predicts an antiferromagnetic interaction of -1.8 cm^{-1} for the 91.56° (average) found in $[Cu_2((R)\text{-}\mathbf{2})Cl_4]$. This prediction is close to the experimentally determined coupling constant, even though there are significant distortions from an ideal square-pyramidal geometry in $[Cu_2((R)\text{-}\mathbf{2})Cl_4]$.

The variable-temperature magnetic data for the homochiral and heterochiral SO_4-bridged copper(II) dimers $[Cu((R)\text{-}\mathbf{4})(\mu^2\text{-}SO_4)]_2$ and $[Cu_2((R)\text{-}\mathbf{4})((S)\text{-}\mathbf{4})(\mu^2\text{-}SO_4)_2]$ are very similar, despite their significantly different core geometries. At 300 K, $\mu_{eff} = 1.85\mu_B$ for both complexes, and at 1.8 K this value drops to $\mu_{eff} = 1.69\mu_B$ and $1.47\mu_B$ for $[Cu((R)\text{-}\mathbf{4})(\mu^2\text{-}SO_4)]_2$ and $[Cu_2((R)\text{-}\mathbf{4})((S)\text{-}\mathbf{4})(\mu^2\text{-}SO_4)_2]$, respectively. There are no maxima in the χ_M vs T plots. By use of the Bleaney−Bowers dimer model on these data sets, the best-fit values of $J = -0.40 \pm 0.03$ cm^{-1} and $g = 2.085 \pm 0.004$ are obtained for $[Cu((R)\text{-}\mathbf{4})(\mu^2\text{-}SO_4)]_2$, while a slightly larger coupling constant of $J = -0.67 \pm 0.02$ cm^{-1} (with $g = 2.078 \pm 0.004$) was found for $[Cu_2((R)\text{-}\mathbf{4})((S)\text{-}\mathbf{4})(\mu^2\text{-}SO_4)_2]$. We suspect that the very weak coupling between the two copper(II) centers in this pair of complexes is due to the relatively large distance between the metal centers as well as the basal/apical geometry.

The magnetic coupling in these SO_4-bridged complexes is intermediate between the coupling found in two other complexes with $\{Cu(\mu\text{-}SO_4)_2Cu\}$ cores reported in the literature. $\{Cu(oaoH_2)(H_2O)(\mu\text{-}SO_4)\}_2$ displays a substantially larger coupling constant of $J = -2.55$ cm^{-1},[22] while $[Cu(PAHOX)(SO_4)]_2 \cdot 2H_2O$ shows a complete lack of coupling.[26] (The structures of these complexes are discussed above.) Together with the data presented in the present report, these results show that the strength of the magnetic interaction between the two copper(II) centers is controlled by the geometry of the $[Cu_2(SO_4)_2]$ core. Although only a limited set of data is available, it appears that the coupling decreases in the order conformation B > A > C (see Figure 10). We tentatively suggest that conformation D would allow the strongest coupling due to the basal/basal geometry; however, unfortunately, relevant magnetic data are not available. A more certain conclusion that can be reached is that the strength of the magnetic coupling can be seen to be dependent on chirality of the ligand. Although in this case only a slight difference in the magnetic coupling was found between the homochiral ($[Cu((R)\text{-}\mathbf{4})(\mu^2\text{-}SO_4)]_2$) and heterochiral ($[Cu_2((R)\text{-}\mathbf{4})((S)\text{-}\mathbf{4})(\mu^2\text{-}SO_4)_2]$) complexes, these results suggest that it should be possible to use the stereochemistry of ligands to alter and perhaps control magnetic interactions in other polynuclear complexes.

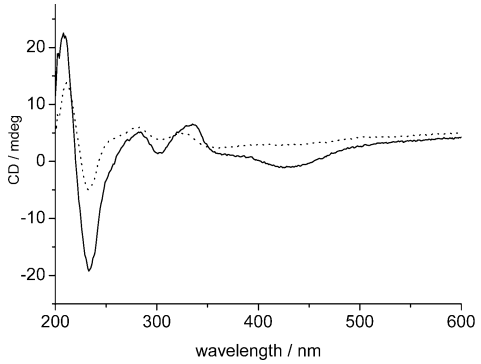

Figure 11. Solid-state spectra of $[Cu_2((R)\text{-}\mathbf{2})Cl_4]$ (dotted line) and $\{Cu((R)\text{-}\mathbf{4})SO_4\}_2$ (solid line), recorded as KBr disks.

Solid-State CD Spectra of the Copper(II) Complexes. The CD spectra of $[Cu_2((R)\text{-}\mathbf{2})Cl_4]$ and $\{Cu((R)\text{-}\mathbf{4})SO_4\}_2$ were measured as KBr disks in a solid-state dedicated CD spectrophotometer.[29] This instrument has been designed to eliminate artifacts due to macroscopic anisotropies (e.g., linear birefringence and linear dichroism) from the measured signal. This enables a true CD spectrum to be obtained.[30] The measured spectra are shown in Figure 11. A negative signal is seen in the visible region of the CD spectrum of $\{Cu((R)\text{-}\mathbf{4})SO_4\}_2$, which has a maximum around 430 nm. This band can be ascribed to the d−d transitions of the copper(II) centers. In the UV region, intense bands are seen for both complexes. The bisignate curve in the 200−250 nm wavelength range is due to exciton coupling of the long axis polarized transitions of the individual naphthyl chromophores. The sign of these couplets (negative at lower energies) is consistent with the R stereochemistry of the binaphthyl ligands.[31]

(26) Bleaney, B.; Bowers, K. D. *Proc. R. Soc. London A* **1952**, *214*, 451.
(27) Rodriguez, M.; Llobet, A.; Corbella, M.; Martell, A. E.; Reibenspies, J. *Inorg. Chem.* **1999**, *38*, 2328.
(28) Rodriguez, M.; Llobet, A.; Corbella, M. *Polyhedron* **2000**, *19*, 2483.
(29) The insolubility of these complexes prevented the measurement of CD spectra in solution.
(30) Kuroda, R.; Harada, T.; Shindo, Y. *Rev. Sci. Instr.* **2001**, *72*, 3802−3810.

Concluding Discussion

We have investigated the coordination chemistry of ligand (*R*)-**2** with $Co(ClO_4)_2$, $Ni(ClO_4)_2$, $CuCl_2$, and $CuSO_4$. During the course of these investigations, we have found that ligand **2** is rather prone to hydrolysis. As a result, we have managed (thus far) to isolate only one complex in which the structure of the ligand is retained, viz., $[Cu_2((R)\text{-}\mathbf{2})Cl_4]$.

The tridentate ligand (*R*)-**4** is the hydrolysis product of (*R*)-**2**, and it exhibits a diverse and interesting coordination chemistry. It was observed that (*R*)-**4** coordinates in a meridional fashion to give $[ML_2]$ complexes of cobalt(II) and nickel(II). The lack of C_2 symmetry in ligand (*R*)-**4** means that the metal centers in these complexes are stereogenic, and thus there are two diastereomers of these complexes. In both cases, however, the complexation reaction appears to be highly diastereoselective with the Λ-$[M((R)\text{-}\mathbf{4})_2](ClO_4)_2$ complex observed in both cases; that is, the axial chirality of the ligand predetermines the stereochemistry of the metal centers.

The dimeric complex$\{Cu((R)\text{-}\mathbf{4})SO_4\}_2$ features a relatively rare $[Cu_2(\mu^2\text{-}(SO_4)_2)]$ core. Interestingly, a different diastereomer of this complex, $[Cu_2((R)\text{-}\mathbf{4})((S)\text{-}\mathbf{4})(SO_4)_2]$, is formed when the synthesis is carried out from racemic starting materials. The formation of this *heterochiral* dimer indicates that the ligands undergo a self-discrimination process based on chirality. This kind of self-discrimination process is rather rare; we are aware of only one other report of this phenomenon in the literature.[20] More commonly, enantiomeric mixtures of *homochiral* products are observed. Indeed, this was seen to be the case for the reaction of *rac*-BINAM, pyridine-2-carboxaldehyde, and $Co(ClO_4)_2$ which produces a racemic mixture of $[Co((R)\text{-}\mathbf{4})_2]^{2+}$ and $[Co((S)\text{-}\mathbf{4})_2]^{2+}$.

Experimental Details

General. ^{1}H NMR spectra were recorded on a JEOL Alpha spectrometer at 500 MHz at 21 °C and were referenced to the residual solvent peak (CD_3CN, $\delta = 1.95$ ppm; CD_3NO_2, $\delta = 4.33$ ppm). ^{13}C NMR were recorded at 125 MHz and were referenced to the residual solvent peak (CD_3CN, $\delta = 1.32$ ppm). UV−Vis absorbance data were recorded on a Shimadzu UV-3150 spectrometer. Solution CD spectra were recorded on a Jasco J720 spectropolarimeter. Solid-state CD spectra were measured as KBr disks on a Jasco J-800KCM spectrophotometer. IR spectra were recorded as KBr disks on a Shimadzu FTIR8000 instrument. ES-MS spectra were recorded on an Applied Biosystems Mariner spectrometer with a flow rate of ca. 5 μL/min and at a concentration in the range $10^{-4}-10^{-6}$ M. Nozzle potentials and temperature (50−70 °C) were kept to a minimum to avoid fragmentation. Microanalyses were performed by Tore Research Center, Eigiyoo, Tokyo. Unless otherwise stated, chemicals were purchased from Wako, TCI, or Aldrich and were used as received. Dried solvents were used for all reactions and measurements.

Magnetic susceptibility data were collected on a Quantum Design SQUID MPMS-XL7 Evercool magnetometer working down to 1.8 K at 1 T field strength. Each sample was measured in a low-background gelcap suspended in a clear straw. The data were corrected for TIP, the diamagnetism of the sample holder, and the constituent atoms by use of Pascal constants.[32]

CAUTION! Perchlorate salts are potentially explosive and should be handled with care and only in small quantities.

Preparation of (*R*)-2. (*R*)-BINAM (360.2 mg, 1.29 mmol) was mixed with pyridine-2-carboxaldehyde (277 mg, 2.58 mmol) in dry CH_2Cl_2 (8 mL). A few 4 Å molecular sieves were added, and the solution was stood at room temperature for 4 days. The sieves were removed, the solution was filtered though a 0.20 μm PTFE membrane filter, and the solvent was removed under reduced pressure. The resulting yellow solid was dried in a vacuum oven overnight at 50 °C. Anal. Calcd (Found) for $C_{32}H_{22}N_4$: C, 83.09 (82.2); H, 4.79 (5.0); N, 12.11 (12.0). ^{1}H NMR (CD_3CN): δ 7.17 (d, 2H, $J = 8.7$ Hz), 7.29−7.32 (m, 4H), 7.44 (t, 2H), 7.47−7.50 (m, 4H), 7.63 (t, 2H), 7.99 (d, 2H, $J = 8.2$ Hz), 8.07 (d, 2H, $J = 8.7$ Hz), 8.43 (s, 2H), 8.53 (m, 2H). ^{13}C NMR (CD_3CN): δ 119.9, 121.6, 126.2, 126.3, 127.1, 127.6, 127.8, 129.1, 130.3, 132.9, 137.6, 148.8, 150.6, 155.4, 162.5 (one peak obscured by the residual solvent peak around 118.2 ppm). ES-MS (CH_3CN/HOAc): $m/z = 463.2$ ($[\mathbf{2} + H]^+$, 100%). UV−Vis (CH_3CN): (λ, ϵ (M^{-1} cm^{-1})) 204 nm (50 100), 226 nm (69 200), 277 nm (41 500). CD (CH_3CN): (λ, $\Delta\epsilon$ (M^{-1} cm^{-1})) 210 nm (51.1), 228 nm (−177.0), 330 nm (−25.0).

$[Cu_2Cl_4((R)\text{-}\mathbf{2})]$. Anhydrous $CuCl_2$ (57.7 mg, 4.30 mmol) was dissolved in dry CH_3OH (1 mL) and added to a stirred solution of (*R*)-**2** (99.33 mg, 2.15 mmol) in CH_2Cl_2 (4 mL). The solution developed a dark brown color, and a yellow-brown solid precipitated from the solution. The reaction mixture was then cooled to −18 °C for 1 h and the solid was filtered off and washed with Et_2O. Yield = 110 mg (66%). X-ray quality crystals could be grown by diffusion of ^{t}BuOMe into a solution of the complex in CH_3OH/CH_2Cl_2 (1/1). Anal. Calcd (Found) for $[Cu_2Cl_4(\mathbf{2})]\cdot CH_3OH$ ($C_{34}H_{28}Cl_4Cu_2N_4O$): C, 48.13 (48.7); H, 3.33 (3.8); N, 6.60 (6.6). ES-MS (acetone): $m/z = 524.9$ ($[Cu(\mathbf{2} - H)]^+$, 20%), 561.9 ($[Cu(\mathbf{2})Cl]^+$, 100%). IR (cm^{-1}): 3435 (br s), 1630 (m), 1595 (m), 1508 (w), 1447 (w), 1304 (w), 1205 (w), 1157 (w), 1024 (w), 818 (m), 775 (m), 752 (m), 419 (m).

$[Ni((R)\text{-}\mathbf{4})_2](ClO_4)_2$. (*R*)-BINAM (63.8 mg, 0.224 mmol) and pyridine-2-carboxaldehyde (24.0 mg, 0.224 mmol) were combined in MeOH (4 mL). $Ni(ClO_4)_2\cdot 6H_2O$ (41.0 mg, 0.112 mmol) was then added to give a red solution. Dark red block-shaped crystals formed when the solution was allowed to stand overnight at room temperature (yield = 63.1 mg). A second crop of crystals were obtained by the slow evaporation of the filtrate at 4 °C (yield = 35.1 mg). The crystals that were used for X-ray crystallography were obtained via a different procedure (see text). Overall yield = 63.1 mg (78%). Anal. Calcd (Found) for $[Ni(\mathbf{4})_2](ClO_4)_2\cdot 4CH_3OH$ ($C_{56}H_{54}Cl_2N_6NiO_{12}$): C, 58.38 (58.9); H, 4.81 (4.6); N, 7.42 (7.2). ES-MS (CH_3OH): $m/z = 402.2$ ($[Ni(\mathbf{4})_2]^{2+}$, 100%), 903.3 ($[Ni(\mathbf{4})_2(ClO_4)]^+$, 32%). UV−Vis ($CH_3OH$): ($\lambda$, ϵ (M^{-1} cm^{-1})) 227 nm (128 000), 282 nm (36 900), 332 nm (19 200), 890 nm (8.5). CD (CH_3OH): λ ($\Delta\epsilon$, (M^{-1} cm^{-1})) 210 nm (256), 229 nm (−210). IR (cm^{-1}): 3433 (br s), 1620 (m), 1591 (m), 1510 (m), 1475 (w), 1437 (w), 1146 (m), 1121 (s), 1109 (s), 1090 (s), 939 (w), 822 (m), 752 (m), 637 (m), 627 (m), 421 (w).

$[Co((R)\text{-}\mathbf{4})_2](ClO_4)_2$. *R*-BINAM (66 mg, 0.232 mmol) and pyridine-2-carboxaldehyde (24.0 mg, 0.224 mmol) were combined in warm MeOH (4 mL). $Co(ClO_4)_2\cdot 6H_2O$ (42.5 mg, 0.116 mmol) was then added to give a red solution. A small number of dark red block-shaped crystals (ca. 15 mg) formed when the solution was allowed to stand overnight at room temperature. These were

(31) Di Bari, L.; Pescitelli, G.; Salvadori, P. *J. Am. Chem. Soc.* **1999**, *121*, 7998−8004.

(32) Kahn, O. *Molecular magnetism*; VCH: Weinheim, Germany, 1993.

Table 1. Crystal Data, Data Collection, and Refinement Parameters

	$[Ni((R)\text{-}4)_2](ClO_4)_2\cdot CH_3NO_2\cdot 0.5CH_3OH$[a]	$[Co((R)\text{-}4)_2](ClO_4)_2\cdot BINAM\cdot 2CH_3OH$	$[Cu_2Cl_4((R)\text{-}2)]\cdot CH_2Cl_2$	$\{Cu_2((R)\text{-}4)(\mu^2\text{-}SO_4)\}_2\cdot xCH_3OH$[b]	$\{Cu_2((R)\text{-}4)((S)\text{-}4)(\mu^2\text{-}SO_4)\}_2\cdot 2CH_3OH$[c]
formula	$C_{53.5}H_{43}Cl_2N_7NiO_{10.5}$	$C_{74}H_{62}Cl_2CoN_8O_{10}$	$C_{33}H_{24}Cl_6Cu_2N_4$	$C_{26}H_{19}CuN_3O_4S$	$C_{56}H_{54}Cu_2N_6O_{12}S_2$
formula wt	1159.64	1353.15	816.34	533.04	1194.25
temp (K)	120(2)	120(2)	100(2)	100(2)	100(2)
crystal system	trigonal	triclinic	monoclinic	trigonal	monoclinic
space group	$P3_121$ (No. 152)	$P1$ (No. 1)	$P2_1$ (No. 4)	$P3_121$ (No. 152)	$P2_1/n$ (No. 14)
a (Å)	11.6939(4)	11.6478(7)	10.001(1)	18.5934(7)	17.688(1)
b (Å)	11.6939(4)	12.4334(7)	13.997(2)	18.5934(7)	8.5915(5)
c (Å)	33.013(2)	13.4116(8)	12.091(2)	16.2207(12)	18.706(1)
α (deg)	90.00	112.265(1)	90.00	90.00	90.00
β (deg)	90.00	98.256(1)	97.520(2)	90.00	115.466(1)
γ (deg)	120.00	98.256(1)	90.00	120.00	90.00
V (Å^3)	3909.7(3)	1573.2(3)	1678.0(4)	4856.4(4)	2566.6(3)
Z	3	1	2	3	2
μ (mm^{-1})	0.550	0.428	1.776	0.767	0.983
reflns meas	24426	9950	10528	30009	15494
reflns obsd ($I > 2\sigma I$)	5110	7728	5861	6888	4949
R_1 ($I > 2\sigma I$)	0.0734	0.0365	0.0450	0.0443	0.0352
wR_2 (all data)	0.213	0.0903	0.1052	0.1100	0.0917
Flack parameter	0.04(2)	0.00(1)	0.03(1)	0.11(1)	N/A

[a] This complex has crystallographic C_2 symmetry. One of the ClO_4^- anions was disordered over two sites (50/50 occupancy ratio). These anions were refined with isotropic thermal parameters. A CH_3OH solvent molecule occupies 50% of the vacant ClO_4^- sites. [b] This complex has crystallographic C_2 symmetry. Disordered solvent molecules (CH_3OH) located in the large channels of the crystal (see text) were modeled as a continuum by use of the SQUEEZE option in PLATON. [c] This complex has crystallographic C_i symmetry.

analyzed by X-ray crystallography and found to contain $[Co((R)\text{-}\mathbf{4})_2](ClO_4)_2\cdot$(*R*)-BINAM (see text). The addition of Et_2O to the mother liquor induced formation of a red crystalline precipitate, which was filtered off and washed with Et_2O. Yield = 60 mg (46%). Anal. Calcd (Found) for $[Co(\mathbf{4})_2](ClO_4)_2\cdot 4CH_3OH$ ($C_{56}H_{54}Cl_2CoN_6O_{12}$): C, 59.37 (59.4); H, 4.80 (4.6); N, 7.42 (7.8). ^{1}H NMR (CD_3NO_2): δ −27.43 (2H), −11.55 (m, 6H), 1.05 (2H), 2.34 (2H), 6.79 (2H), 7.38 (2H), 8.55 (2H), 11.37 (2H), 13.07 (2H), 21.50 (2H), 23.95 (2H), 57.08 (2H), 69.99 (2H). ES-MS (CH_3OH): m/z = 402.5 ($[Co(\mathbf{4})_2]^{2+}$, 100%), 904.0 ($[Co(\mathbf{4})_2(ClO_4)]^+$, 3%). UV−Vis ($CH_3OH$): ($\lambda$, ϵ (M^{-1} cm^{-1})) 239 nm (132 900), 282 nm (31 700), 342 nm (9450), 980 nm (17.2). CD (CH_3OH): λ ($\Delta\epsilon$, (M^{-1} cm^{-1})) 210 nm (57.7), 27 nm (20.6), 248 nm (−153), 273 nm (−43.4), 341 nm (−37.5), 400 nm (sh, −15.0). IR (cm^{-1}): 3433 (br s), 1618 (m), 1593 (m), 1508 (m), 1123 (s), 1109 (s), 1020 (w), 928 (w), 820 (m), 750 (m), 637 (m).

***rac*-$[Co(\mathbf{4})_2](ClO_4)_2$.** *rac*-BINAM (82.8 mg, 0.291 mmol) was combined with pyridine-2-carboxaldehyde (31.2 mg, 0.291 mmol) in MeOH (5 mL). $Co(ClO_4)_2\cdot 6H_2O$ (53.0 mg, 0.145 mmol) was then added to give a red-orange solution, which was stirred at room temperature for 30 min. The solution was then cooled to −18 °C overnight to give an orange precipitate, which was filtered off, washed with cold MeOH and Et_2O, and air-dried. The filtrates were combined and cooled to −18 °C to give a second crop of product. Total yield = 106 mg (73%). An analytically pure product was obtained by recrystallization from a minimum of hot MeOH. Anal. Calcd (Found) for $[Co(\mathbf{4})_2](ClO_4)_2\cdot 4CH_3OH\cdot H_2O$ ($C_{56}H_{56}Cl_2CoN_6O_{13}$): C, 58.44 (58.3); H, 4.90 (4.3); N, 7.30 (7.6). ^{1}H NMR (CD_3NO_2): δ −27.31 (2H), −11.55 (m, 6H), 1.03 (2H), 2.40 (2H), 7.20 (2H), 7.83 (2H), 8.64 (2H), 11.37 (2H), 13.07 (2H), 21.43 (2H), 23.90 (2H), 56.94 (2H), 69.79 (2H). ES-MS (CH_3OH): m/z = 402.7 ($[Co(\mathbf{4})_2]^{2+}$, 100%), 904.3 ($[Co(\mathbf{4})_2(ClO_4)]^+$, 26%). UV−Vis ($CH_3OH$): ($\lambda$, ϵ (M^{-1} cm^{-1})) 239 nm (137 000), 281 nm (34 100), 343 nm (10 650), 980 nm (17.5). IR (cm^{-1}): 3423 (br s), 1618 (m), 1593 (m), 1508 (m), 1474 (m), 1146 (m), 1121 (s), 1109 (s), 1089 (s), 1018 (w), 820 (m), 750 (m), 637 (m), 627 (m).

$\{Cu((R)\text{-}4)(\mu^2\text{-}SO_4)\}_2$. (*R*)-BINAM (105.5 mg, 0.372 mmol) was combined with pyridine-2-carboxaldehyde (39.8 mg, 0.372 mmol) in CH_3OH (5 mL). $CuSO_4\cdot 5H_2O$ (92.8 mg, 0.372 mmol) was then added, and the reaction mixture was put in a closed vial, sonicated, and then stood on a hot plate at 50 °C overnight. A mixture of small dark brown crystals and a brown precipitate formed. Yield = 192 mg (97%). The complex could be recrystallized by the slow diffusion of Et_2O into a CH_3OH solution. The crystals that were used for X-ray crystallography, however, were formed by combining equimolar samples of anhydrous $CuSO_4$ and (*R*)-**2** in dry CH_3OH, and standing the resulting suspension on a 50 °C hot plate in a closed vial for 3 days. Anal. Calcd (Found) for $[Cu_2(\mathbf{4})_2(SO_4)_2]\cdot 7CH_3OH$ ($C_{59}H_{66}Cu_2N_6O_{15}S_2$): C, 54.92 (54.5); H, 5.16 (4.7); N, 6.51 (6.7). IR (cm^{-1}): 3433.1 (br s), 1624 (m), 1597 (m), 1508 (m), 1304 (w), 1190 (m), 1117 (s), 1026 (m), 941 (w), 818 (m), 750 (m), 619 (m), 503 (w), 419 (w).

$\{Cu_2((R)\text{-}4)((S)\text{-}4)(\mu^2\text{-}SO_4)\}_2$. *rac*-BINAM (68.9 mg, 0.242 mmol) was combined with pyridine-2-carboxaldehyde (26.0 mg, 0.242 mmol) in CH_3OH (3 mL). $CuSO_4\cdot 5H_2O$ (60.5 mg, 0.242 mmol) was then added, and the reaction mixture was put in a closed vial, sonicated, and then stood on a hot plate at 50 °C overnight. A mass of dark brown block-shaped crystals formed, which were filtered off, washed with Et_2O, and air-dried. Yield 130 mg (90%). Anal. Calcd (Found) for $[Cu_2(\mathbf{4})_2(SO_4)_2]\cdot 4CH_3OH$ ($C_{56}H_{54}Cu_2N_6O_{12}S_2$): C, 56.32 (55.8); H, 4.56 (4.2); N, 7.04 (7.1). IR (cm^{-1}): 3433.1 (br s), 1624 (m), 1597 (m), 1508 (m), 1306 (w), 1186 (m), 1119 (s), 1028 (m), 941 (w), 820 (m), 752 (m), 621 (m), 503 (w), 419 (w).

Crystallography. X-ray data were collected on a Bruker APEX system (CCD detector) at 100−120 K with Mo Kα radiation (0.710 73 Å) and are shown in Table 1. All data were corrected for Lorentzian, polarization, and absorption. All structures were solved by direct methods (SHELXS-97) and refined against $|F|^2$ by use of anisotropic thermal displacement parameters for all non-hydrogen atoms (SHELXL-97). All hydrogen atoms attached to carbon atoms were placed in calculated positions. Other hydrogen atoms were located on the electron density difference maps.

Acknowledgment. D.B.L. is grateful to NSERC of Canada for research support. J.L. is the recipient of a graduate fellowship from FQRNT of Quebec.

Supporting Information Available: Crystallographic data in CIF format. This material is available free of charge via the Internet at http://pubs.acs.org.

IC049910Y